



Impact of Ferro-Geopolymer Encapsulation on the Structural Integrity of Concrete Columns Under Axial Load

K. Rama Krishna Reddy* , D. Rajkumar 

Department of Civil & Structural Engineering, Faculty of Engineering and Technology, Annamalai University, Annamalaiagar 608002, India

Corresponding Author Email: k.ramakrishnareddy3949@gmail.com

Copyright: ©2025 The authors. This article is published by IETA and is licensed under the CC BY 4.0 license (<http://creativecommons.org/licenses/by/4.0/>).

<https://doi.org/10.18280/rcma.350209>

ABSTRACT

Received: 6 February 2025

Revised: 11 March 2025

Accepted: 26 March 2025

Available online: 30 April 2025

Keywords:

ferro-geopolymer, compressive strength, sorptivity, concrete column, structural integrity, optimal mix proportions, ductility indices

This research explores the impact of ferro-geopolymer encapsulation on the axial load-bearing capacity and structural integrity of concrete columns. Ferro-geopolymer, a composite material that merges ferrocement and geopolymer technology, offers potential advantages in enhancing the mechanical properties of concrete. Experimental tests were performed on columns encapsulated with ferro-geopolymer jackets, subjected to axial compression and also studied the slump cone test on fresh state concrete, compressive strength and sorptivity test were conducted on hardened concrete. Results indicated significant improvements in compressive strength compared to unreinforced columns. The encapsulation provided effective confinement, delaying cracking and increasing ultimate load capacity. Slump cone test showed higher value with 100% of fly ash addition. F50G50 mix showed higher compressive strength values at 7, 28 and 90 days of 29.77MPa, 45.72MPa and 46.19MPa, respectively. G100 mix showed lower sorptivity values compared to all mixes. Three layers of expanded and wire mesh showed better load carrying capacity, higher deflection ductility index and more energy ductility index values under axial loading. The findings suggest that ferro-geopolymer encapsulation is a promising technique for retrofitting and strengthening concrete columns, offering a sustainable and efficient solution for improving structural resilience.

1. INTRODUCTION

The large-scale production of cement has significantly increased carbon dioxide (CO₂) levels in the atmosphere, making it a major contributor to greenhouse gas emissions. Concrete, which comes second only to water as the most widely used material on Earth, mainly relies on Ordinary Portland Cement (OPC) as its key ingredient. Manufacturing OPC consumes substantial natural resources, mainly limestone, along with various supplementary materials such as fly ash (FA), ground granulated blast furnace slag (GGBS), and rice husk ash (RHA). It is high-temperature breakdown of limestone that releases CO₂ in huge amounts in the process of manufacturing. The amount of electricity required, in conjunction with the extremely high-energy costs for the manufacture of clinker, leads to CO₂ emissions ~1 tonne/tonne of OPC generated. With the growing urgency to combat environmental damage, researchers and engineers are actively exploring sustainable alternatives to conventional cement-based concrete. Materials like fly ash and GGBS have shown great potential as substitutes, offering lower carbon footprints and improved durability [1].

A appropriate methodology involves the utilization of geopolymer binder, created by amalgamating high-silica an alumina-rich substances with an alkaline activator including

sodium or potassium silica and hydroxide. The remarkable strength and durability properties of Geopolymers, along with their potential to avoid high carbon footprints, offer the potential for better sustainable construction techniques than those possible with more traditional OPC binders [2-4]. Ferro-geopolymer, a novel composite material, was inspired from the known ferrocement technique by the application of geopolymer mortar in the composite wherein wire mesh was used as reinforcement. Invented by Joseph Louis Lambot in 1848, Ferrocement has been widely used for many structural applications, including boats, water tanks, water silos, pipes, floating structures, roofing slabs, beams, lintels and irrigation channels [5, 6].

Ferrocement comprises a cement-sand mortar matrix reinforced with mesh, which may be constructed from metallic or non-metallic elements. This composite demonstrates elevated tensile strength, ductility, durability, and an exceptional strength-to-weight ratio. Consequently, ferrocement components are generally smaller, lighter, and more economical than conventional reinforced concrete elements. The incorporation of geopolymer technology in ferrocement construction improves sustainability by decreasing cement usage and minimizing CO₂ emissions, all while preserving structural integrity.

Ferrocement has long been recognized for its ability to form

lightweight structural elements with excellent crack resistance and high tensile strength, owing to the use of thin mortar layers reinforced with multiple layers of fine wire mesh. Its performance under various loading conditions has made it a popular choice in thin-shell structures, precast elements, and retrofitting applications. On the other hand, geopolymer binders-produced by the alkali activation of aluminosilicate-rich materials such as fly ash, slag, or metakaolin-have gained attention as an environmentally friendly alternative to Portland cement. Geopolymers exhibit desirable properties such as high early strength, low shrinkage, and excellent chemical and thermal resistance.

Recent studies have explored the integration of ferrocement and geopolymer materials, focusing on axial load performance. El-Sayed et al. [7] investigated the axial compression behavior of high-strength geopolymer ferrocement columns, demonstrating that incorporating wire mesh reinforcement enhances load-bearing capacity and ductility. El-Sayed [8] examined the structural behavior of ferrocement geopolymer high-strength concrete (HSC) columns subjected to axial loading. The research utilized rice straw ash (RSA) as a binding material and tested different reinforcement types, including expanded and welded wire meshes. The findings indicated that welded wire mesh improved ultimate failure load by approximately 28.10% compared to expanded wire mesh. Makhoul et al. [9] examined high-strength geopolymer ferrocement columns under axial loads, confirming that increased layers of steel welded wire mesh improve structural performance. Additionally, Karakoç et al. [10] optimized the mechanical properties of geopolymer ferrocement by adjusting binder compositions and alkaline activator ratios, achieving significant improvements in compressive, shear, and flexural strengths. These findings collectively suggest that the strategic combination of ferrocement and geopolymer materials can enhance the axial load performance of structural elements.

Krishna et al. [11] explored the effects of ferrocement confinement and fiber-reinforced concrete cores on axial load performance. Results showed that ferrocement wrapping significantly enhanced load-carrying capacity, with fiber-reinforced ferrocement increasing load capacity by 51%, while non-fibrous ferrocement improved it by 43% compared to conventional reinforced concrete columns.

2. MATERIALS

2.1 Cement

The current study employed Ordinary Portland cement of

53 grade, conforming to IS: 12269-2013 [12], with a particle size of 90µm. The specific gravity was 3.12, and the standard consistency was 32%.

2.2 River sand

River sand, locally sourced and compliant with Zone-II specifications according to IS: 383-2016 [13], was utilized. The sand's bulk density, specific gravity, and fineness modulus were 1.41g/cc, 2.68, and 2.9, respectively.

2.3 Crushed granite

Crushed granite aggregate with a maximum size of 16mm, compliant with IS: 383-2016 [13], was employed. The coarse aggregate exhibited a bulk density of 1.46g/cc, a specific gravity of 2.7, and a fineness modulus of 7.1.

2.4 Fly ash

Class F fly ash, according to IS: 3812: (Part-II)-2003 [14], sourced from the Ramagundam thermal power plant in India, exhibited a specific gravity of 2.18 and a fineness of 6422cm²/g.

2.5 Superplasticizer

A superplasticizer based on modified polycarboxylate ether, compliant with IS 9103-2004 [15], was employed. The product is named Armix Hyyecrete PC 20. Multiple experimental mixtures established the optimal dosage.

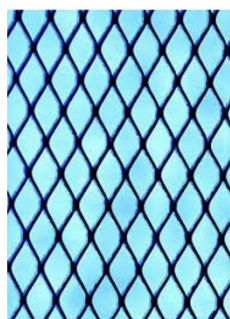
2.6 Ground granulated blast furnace slag (GGBS)

The GGBS utilized complied with ASTM C 989 [16] and was provided by a reputable manufacturer of GGBS.

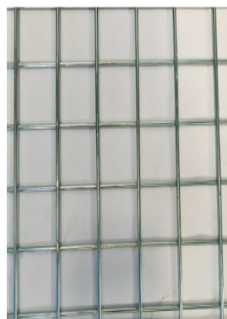
2.7 Alkali solution

The ratio of sodium silicate to sodium hydroxide (Na₂SiO₃/NaOH) was kept at 2.5. Both of the solutions were acquired from chemical sources located in the immediate vicinity. NaOH was acquired in the form of flakes, and then it was dissolved in water that had been distilled. Our choice for the molarity of NaOH was 12M. The preparation of the alkaline solution took place twenty-four hours prior to the casting of the geopolymer mortar.

2.8 Steel reinforcement



Expanded metal mesh (EMM)



Welded wire mesh (WWM)

Figure 1. Expanded metal mesh and welded wire mesh

Table 1. Mechanics of meshes

Type of Mesh	Opening Size (mm)	Weight (gm/m ²)	Diameter (mm)	Yield Tensile Strength (MPa)	Ultimate Tensile strength (MPa)	Modules of Elasticity (Gpa)
EMM	19*33	17	1.5*2.1	225	334	136
WWM	12*12	4.2	0.75	379	598	171

In the M25 RC column, the primary reinforcement comprised steel bars with a diameter of 12 millimeters (Fe500), while the lateral ties consisted of steel with a diameter of 6 millimeters. For the purpose of providing reinforcement in ferrogeopolymer mortar, expanded metal mesh (EMM) and welded wire mesh (WWM) were utilized, as illustrated in Figure 1. The mechanical properties of steel bars and steel meshes is presented in Table 1.

3. MIX PROPORTIONS

In current study, geopolymer mortar has taken with density of 2100kg/m³. The quantities of binder ingredients (FA and GGBS), fine aggregate, and alkaline liquids (Na₂SiO₃ and NaOH) were determined by means of geopolymer mortar

density. Assumed a binder to fine aggregate ratio of 1:1.5 and an alkaline liquid to binder ratio of 0.4. The sodium hydroxide concentration is kept at 12M. Table 2 shows the mix ratios of cement mortar and geopolymer mortar, more especially the different percentages of binder components. The IS Code design [17] approach was followed in formulating the concrete mix including ordinary Portland cement (OPC). The mix design for M25 grade concrete consists of carefully proportioned materials to achieve the desired strength and durability. The quantities utilized in this mix are cement, water, fine aggregate and coarse aggregate of 359kg/m³, 154kg/m³, 740kg/m³, and 1267kg/m³, respectively. Additionally, a chemical admixture of 3.53kg/m³ is incorporated. The mix maintains a water-cement ratio of 0.43 to ensure proper consistency. The final mix proportion by weight is 1: 2.06: 3.52, ensuring a balanced composition for concrete production.

Table 2. Mix proportion of mortar specimens

Cementitious Material	FA (kg/m ³)	GGBS (kg/m ³)	Sand (kg/m ³)	NaOH (kg/m ³)	Na ₂ SiO ₃ (kg/m ³)	Alkaline liquid (kg/m ³)	Water (kg/m ³)	Na ₂ SiO ₃ /NaOH
FA 100%	724.12	-	1086.20	82.76	206.89	289.65	72.41	
GGBS 100%	-	724.12	1086.20	82.76	206.89	289.65	72.41	2.5
FA50% GGBS50% C100%	362.06	362.06	1086.20	82.76	206.89	289.65	72.41	
Cement: Sand=1:3								

4. EXPERIMENTAL DESIGN

The experimental study was carried out in four phases as shown in Figure 2.

Phase 1 involved the preparation of nine geopolymer mortar cubes (70.6mm×70.6mm×70.6mm) to evaluate the compressive strength. In Phase 2, a M25 grade reinforced concrete (RC) square column (150mm×150mm×1500mm) was cast and subjected to ultimate load testing, with the mix proportion details provided in Table 2 and column specifications in Table 3. Phase 3 involved the preparation of six additional M25 grade RC columns (150mm×150mm×1500mm), which were subjected to 80% of the ultimate load to induce damage. In Phase 4, these six damaged RC columns were strengthened using ferro-geopolymer jacketing with the optimum mortar mix (F50G50). The jacketing was applied along the full height of the columns, leaving a 20mm gap at both ends to prevent direct loading on the ferro-geopolymer mesh. The reinforcement details of the conventional and retrofitted RC columns are illustrated in Figure 3. The specimens were cured in a controlled environment at 27±2°C with a relative humidity of 90±5% for 28 days. Standard water curing was maintained to ensure proper geopolymerization and hydration of the concrete jacketing. Corrosion protection for steel meshes

(EMM/WWM) was ensured by applying a zinc-rich anti-corrosion coating before use them in concrete jacketing.

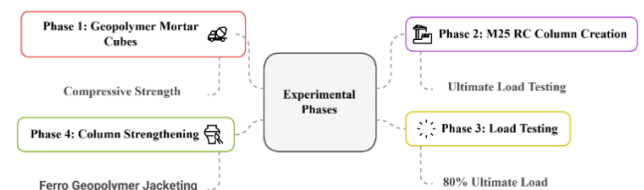
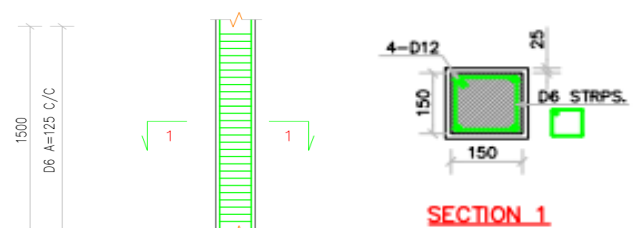
**Figure 2.** Experimental program in different phases**Figure 3.** Reinforcement details of conventional RC column specimens

Table 3. Details of RC column

Materials	Quantity
Grade of concrete	M25
Grade of steel	Fe500
Area of column	22500 mm ²
Area of main steel	452.35 mm ²
Lateral ties	6 mm dia, 125 mm dia
Ultimate load	376.54 kN
80% of ultimate load	301.23 kN

5. METHODS

5.1 Workability

The slump cone test is used to determine the consistency of the freshly mixed concrete. The workability of fresh concrete was evaluated through the use of a standard slump cone in accordance with IS 1199-2018 [18]. This test was carried out in order to determine the feasibility of the concrete.

5.2 Cube compressive strength

The compressive strength test was performed after curing period of 7, 28 and 90 days. Cube specimens measuring 150×150×150mm were tested following the IS 516:1959 [19] standards.

5.3 Sorptivity test

In the Sorptivity Test, water absorption through capillary action is evaluated. After being oven-dried, concrete discs measuring 100mm×50mm are weighed (W_0) and then partially submerged in water with a depth of 5mm. Weight, denoted by W_t , is measured at regular intervals, and the sorptivity, denoted by S , is determined by the following formula:

$$S = \frac{\Delta W}{A \times \sqrt{t}}$$

6. RESULTS AND DISCUSSION

6.1 Slump cone method

Table 4 shows that slump cone test values for the mix proportions of F100, G100, F50G50 and C100. For the mix F100, the slump value is 105mm, indicating that this mix has high workability and can be easily placed and finished. On the other hand, the mix G100 has a slump value of 71mm, which signifies moderate workability. The F50G50 mix, which combines the F and G components in equal proportions, has a slump value of 77mm, showing a middle ground in terms of workability between the F100 and G100 mixes. Lastly, the mix C100 has a slump value of 79mm, also suggesting moderate workability.

The workability characteristics of geopolymer mortar compositions vary significantly based on their Fly Ash and GGBS content. While Fly Ash contributes to enhanced workability, GGBS typically results in a reduction. Notably, traditional cement-based mortar fails to attain the superior workability levels observed in geopolymer mixtures composed solely of Fly Ash.

Table 4. Cone slump results

Mix ID	Slump Value In Mm	Type of Slump
F100	105	True Slump
G100	71	True Slump
F50G50	77	True Slump
C100	79	True Slump

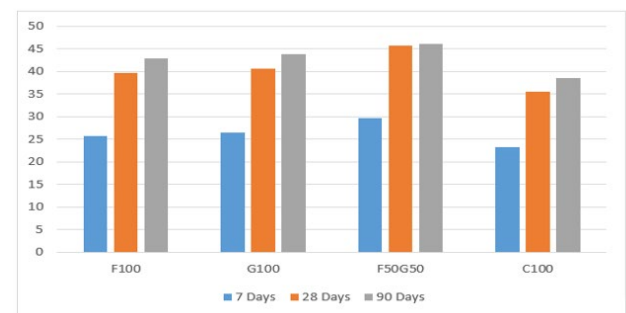
6.2 Compressive strength

This study presents the compressive strength test results of various mortar specimens at 7, 28, and 90 days, as depicted in Figure 4. The examined mixtures comprise Fly Ash (F), Ground Granulated Blast Furnace Slag (GGBS) (G), and Cement (C). Notably, F100, G100, and F50G50 represent geopolymer-based compositions, whereas C100 serves as the conventional cement mortar control. The analysis focuses on the development of strength in these mixtures over time.

At the 7-day, geopolymer mortars exhibited superior strength compared to cement mortar. The F50G50 mixture achieved the highest early strength at 29.77MPa, surpassing C100 (23.33MPa) by 27.63%. Additionally, G100 (26.47MPa) demonstrated better early strength than F100 (25.76MPa), underscoring the significant contribution of GGBS to early strength gain relative to Fly Ash. These findings indicate that geopolymers develop strength more rapidly than conventional cement mortar.

By the 28-day, geopolymer mortars continued to demonstrate superior performance. The F50G50 mix retained its leading position with a compressive strength of 45.72MPa, exceeding C100 (35.53MPa) by 28.72%. Similarly, G100 (40.64MPa) slightly outperformed F100 (39.66MPa), further reinforcing the role of GGBS in enhancing compressive strength. These results confirm the efficacy of geopolymer mortars as robust alternatives for construction applications.

At curing age of 90 days, the trend of strength development was consistent, and geopolymer mixtures were at the forefront. The compressive strength of the F50G50 mix attained 46.19MPa that exceeded C100 (38.52MPa) with a value of 19.91%. Both F100 (42.88MPa) and G100 (43.91MPa) also showed a great improvement compared with C100, proving the excellent long-term strength characteristics of geopolymer mortars.

**Figure 4.** Compressive strength values of mortar

In summary, the results underscore the superior strength performance of geopolymer mortars at all tested ages. The F50G50 mixture consistently achieved the highest compressive strength, making it the most promising alternative to conventional cement mortar. This enhanced performance is attributed to the pozzolanic reaction of Fly Ash

and the high reactivity of GGBS, which expedite strength development. Conversely, C100 exhibited slower strength gain and lower overall compressive strength, reaffirming the advantages of geopolymer mortars in construction applications.

6.3 Sorptivity test

The results of the sorptivity test provide valuable insights into how different mortar types absorb water through capillary action, which is a key factor in determining their durability as shown in Figure 5. Lower sorptivity values indicate better resistance to moisture ingress, thereby enhancing long-term performance.

The tested mortars showed, the one with the highest sorptivity was based on cement (C100) having it equal to 0.087 mm/√s, and reflecting that is a more porous structure, limiting to the absorption of water. The Fly Ash-based geopolymer mortar (F100) showed 17.24% reduction in sorptivity (0.072mm/√s) when compared to C100. This results from a dense microstructure that is generated through geopolymerization, reducing capillary pores and inhibiting water transport.

The GGBS-based geopolymer mortar (G100) performed even better, with a sorptivity value of 0.067mm/√s, representing a 22.99% reduction from C100. This superior performance is likely due to the higher reactivity of GGBS, which results in a more compact and less permeable structure. Additionally, the hybrid geopolymer mortar (F50G50), which is a mix of Fly Ash and GGBS, exhibited a 14.94% reduction in sorptivity (0.074mm/√s) compared to C100.

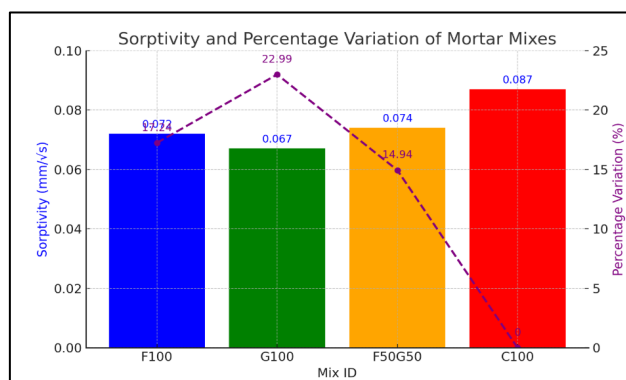


Figure 5. Sorptivity values of mortar mixes

This value is slightly higher than that of F100 and G100, but it indicates a much higher water absorption resistance than traditional cement mortar. In general, the obtained results prove that geopolymer mortars are more resistant to moisture than conventional cement mortar, thus providing better

durability. Out of all the geopolymer mortars studied, the GGBS-based mix (G100) possessed the lowest sorptivity, and was therefore the most resistant to water ingress. The F50G50 mix also performed well, indicating that combining Fly Ash and GGBS can further optimize durability. These findings underscore the potential of geopolymer mortars as a superior alternative to cement-based mortars, particularly for applications where moisture resistance is crucial.

7. DISCUSSION ON TEST RESULTS OF COLUMN SPECIMENS

Under load, the structural behaviour of reinforced concrete (RC) columns is evaluated based on compressive strength and ductility performance. In this work, RC columns were retrofitted (after 80% of ultimate load) with welded wire meshes (W), integrating expanded meshes (E) and ferropolymer meshes (FG). Important structural characteristics guided the analysis of the experimental data.

7.1 Load carrying capacity

Table 5 shows the load and deflection values for first crack, yield and ultimate under axial load condition. Three stages i.e., first crack, yield, and ultimate load were used to evaluate the columns' load-carrying capacity. With an ultimate load of 606.54kN, the conventional column (CC) shown the lowest load-bearing capacity at every step. Strength of the columns was much enhanced by retrofitting with ferropolymer meshes. With three layers of welded wire mesh, FGW3 (among all the retrofitted specimens) obtained the maximum ultimate load of 1624.51kN, about 2.7 times more than the strength of the CC column. Analogous to this, FGE3 (three layers of expanded wire mesh) showed an ultimate load of 1584.32kN, proving that several layers of ferropolymer meshes greatly improve load resistance. Increasing the number of FG mesh layers seems to reinforce the column by enhancing confinement and crack resistance [20].

Table 6 presents the ductility indices for different mix proportions of column specimens. The Deflection Ductility Index and the Energy Ductility Index are measured for all column specimens. The conventional column (CC) has the lowest values, with a deflection ductility index of 2.54 and an energy ductility index of 19.84. The other columns, labeled FGE1 to FGE3 and FGW1 to FGW3, show improved ductility indices, indicating better deformation capacity and energy absorption. Among them, FGE3 exhibits the highest ductility indices (4.2 for deflection and 32.06 for energy), suggesting superior performance. The trend indicates that modifications in the material composition or reinforcement of these columns positively influence their ductility characteristics.

Table 5. Experimental test results on columns

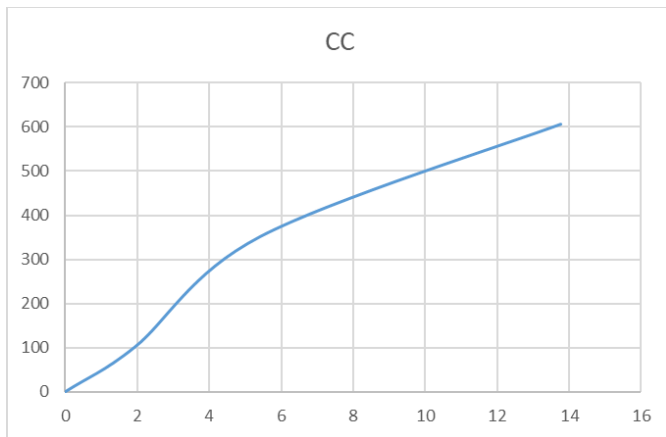
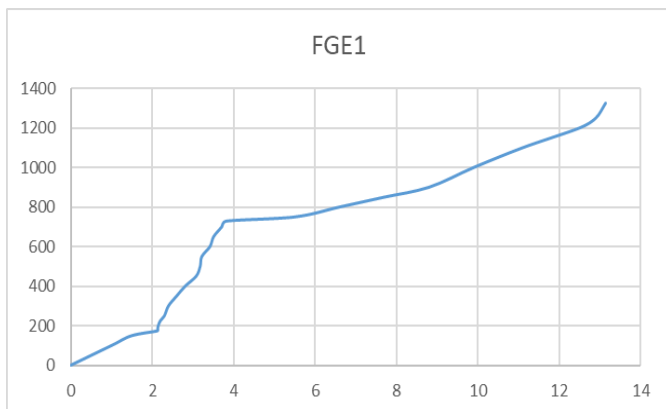
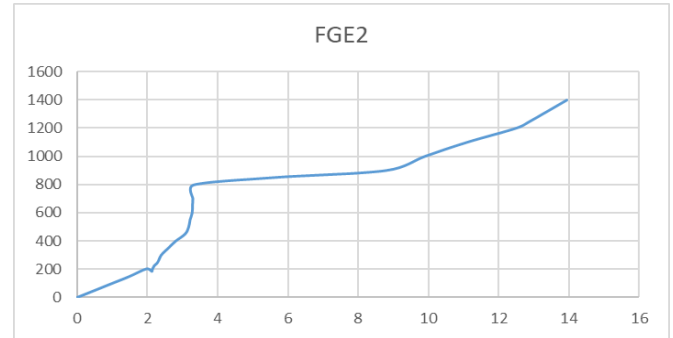
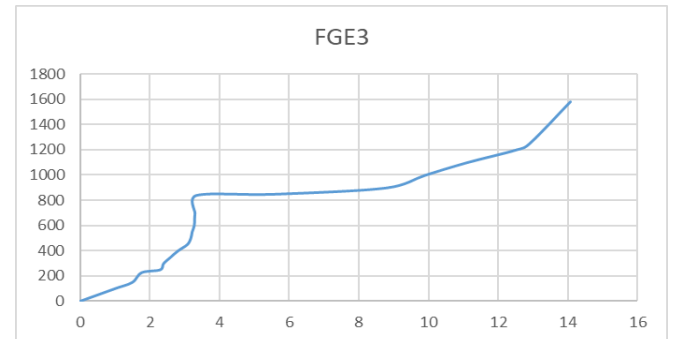
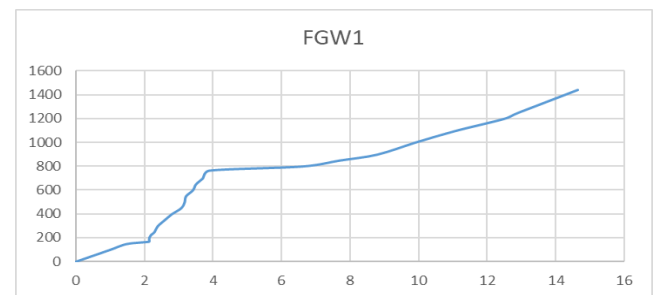
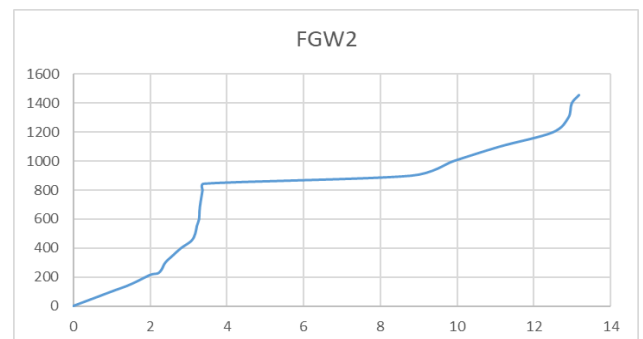
Column ID	First Crack		Yield		Ultimate	
	Load (kN)	Deflection (mm)	Load (kN)	Deflection (mm)	Load (kN)	Deflection (mm)
CC	101.12	1.93	351.79	5.42	606.54	13.78
FGE1	174.19	2.13	728.75	3.81	1325.09	13.14
FGE2	203.35	1.98	797.33	3.32	1398.84	13.94
FGE3	227.41	1.77	841.61	3.35	1584.32	14.08
FGW1	168.84	2.14	765.11	3.9	1442.33	14.64
FGW2	215.4	2.01	844.78	3.4	1456.79	13.18
FGW3	251.51	1.93	926.93	4.08	1624.51	15.97

Table 6. Deflection and energy ductility test results

Column ID	Deflection Ductility Metrics	Energy Ductility Metrics
CC	2.54	19.84
FGE1	3.44	20.82
FGE2	4.19	29.48
FGE3	4.2	32.06
FGW1	3.75	21.74
FGW2	3.87	26.27
FGW3	3.91	31.31

7.2 Load vs deflection behavior

Figures 6-12 show the load Vs deflection behaviour of different mix proportions of column specimens. Initially, the deflection of the columns was measured under circumstances of yield, ultimate load, and first crack. Brittle behaviour was shown by the CC column recording an ultimate deflection of 13.78mm and a yield deflection of 5.42mm. Reduced yield deflection of retrofitted columns suggested higher rigidity under load. Their final deflections were much higher, nevertheless, indicating better deformation capacity prior to collapse. With an ultimate deflection of 15.97mm, FGW3 had the greatest retrofitted specimen; followed by FGW1 (14.64mm) and FGE3 (14.08mm). These results imply that, allowing columns to sustain more deformations before failure, welded wire mesh (FGW series) offers better flexibility than expanded wire mesh (FGE series). For structural uses in seismic-prone areas, where increased ductility and energy dissipation are absolutely necessary, this behaviour is very beneficial [21].

**Figure 6.** Load-Deflection for CC**Figure 7.** Load-Deflection for FGE1**Figure 8.** Load-Deflection for FGE2**Figure 9.** Load-Deflection for FGE3**Figure 10.** Load-Deflection for FGW1**Figure 11.** Load-Deflection for FGW2

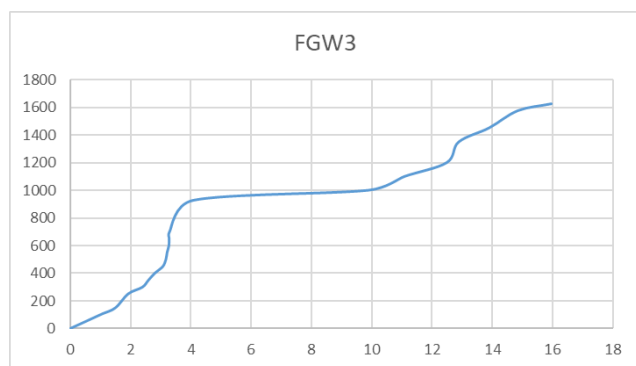


Figure 12. Load-Deflection for FGW3

8. CONCLUSION

This study investigates the structural performance of concrete columns reinforced with ferro-geopolymer jackets when subjected to axial compressive loads. The ferro-geopolymer mix was designed using 100% fly ash, which demonstrated superior workability in the slump cone test, facilitating better placement and compaction of the material.

Among the tested mix designs, the F50G50 mix (a combination of 50% fly ash and 50% GGBS) achieved the highest compressive strength at various curing ages—29.77MPa at 7 days, 45.72MPa at 28 days, and 46.19MPa at 90 days—indicating a significant gain in strength over time. Conversely, the G100 mix (100% GGBS) exhibited the lowest sorptivity values, signifying improved durability due to reduced water absorption and permeability. The structural integrity of the columns was further enhanced by incorporating three layers of expanded metal mesh (EMM) and welded wire mesh (WWM). This reinforcement significantly improved the load-carrying capacity and deflection ductility index which are critical parameters in assessing the ductility and toughness of columns under axial compression. Overall, the results suggest that ferro-geopolymer encapsulation is an effective and environmentally friendly retrofitting technique for strengthening concrete columns. This method not only enhances structural resilience but also contributes to sustainability by utilizing industrial by-products like fly ash and GGBS, reducing reliance on conventional cement-based materials. Future research should focus on evaluating the seismic performance of ferro-geopolymer-encapsulated columns, including energy dissipation, ductility, and behavior under cyclic loading. Optimizing reinforcement could further improve stability. Additionally, a cost-benefit analysis is needed to assess practical viability by comparing material costs, durability, maintenance, and environmental impact. Prior studies suggest potential savings and performance benefits, supporting the feasibility of this sustainable structural solution.

REFERENCES

- [1] Pacheco-Torgal, F., Castro-Gomes, J.P., Jalali, S. (2008). Adhesion characterization of tungsten mine waste geopolymeric binder. Influence of OPC concrete substrate surface treatment. *Construction and Building Materials*, 22(3): 154-161. <https://doi.org/10.1016/j.conbuildmat.2006.10.005>
- [2] Kavyateja, B.V., Jawahar, J.G., Sashidhar, C., Panga, N.R. (2021). Moment carrying capacity of RSCC beams incorporating alccofine and fly ash. *Pollack Periodica*, 16(1): 19-24. <https://doi.org/10.1556/606.2020.00231>
- [3] Chindaprasirt, P., Chalee, W. (2014). Effect of sodium hydroxide concentration on chloride penetration and steel corrosion of fly ash-based geopolymer concrete under marine site. *Construction and Building Materials*, 63: 303-310. <https://doi.org/10.1016/j.conbuildmat.2014.04.010>
- [4] Zhang, Z., Yao, X., Zhu, H. (2010). Potential application of geopolymers as protection coatings for marine concrete: I. Basic properties. *Applied Clay Science*, 49(1-2): 1-6. <https://doi.org/10.1016/j.clay.2010.01.014>
- [5] Chindaprasirt, P., Rattanasak, U. (2016). Improvement of durability of cement pipe with high calcium fly ash geopolymer covering. *Construction and Building Materials*, 112: 956-961. <https://doi.org/10.1016/j.conbuildmat.2016.03.023>
- [6] Kaish, A.B.M.A., Jamil, M., Raman, S.N., Zain, M.F.M. (2015). Axial behavior of ferrocement confined cylindrical concrete specimens with different sizes. *Construction and Building Materials*, 78: 50-59. <https://doi.org/10.1016/j.conbuildmat.2015.01.044>
- [7] El-Sayed, T.A., Deifalla, A.F., Shaheen, Y.B., Ahmed, H. H., Youssef, A.K. (2023). Experimental and numerical studies on flexural behavior of GGBS-based geopolymer ferrocement beams. *Civil Engineering Journal*, 9(3): 629-653.
- [8] El-Sayed, T.A. (2021). Axial compression behavior of ferrocement geopolymer HSC columns. *Polymers*, 13(21): 3789. <https://doi.org/10.3390/polym13213789>
- [9] Makhlof, M.H., Alaa, M., Khaleel, G.I., Elsayed, K.M., Mansour, M.H. (2024). Shear behavior of reactive powder concrete ferrocement beams with light weight core material. *International Journal of Concrete Structures and Materials*, 18(1): 46. <https://doi.org/10.1186/s40069-024-00684-x>
- [10] Karakoç, M.B., Türkmen, İ., Maraş, M.M., Kantarci, F., Demirboğa, R., Toprak, M.U. (2014). Mechanical properties and setting time of ferrochrome slag based geopolymer paste and mortar. *Construction and Building Materials*, 72: 283-292. <https://doi.org/10.1016/j.conbuildmat.2014.09.021>
- [11] Krishna, A., Sreekumaran, S., Kaliyaperumal, S.R.M., Shreemathi. (2024). Performance evaluation of axially loaded high strength ferrocement confined fibre reinforced concrete columns. *Innovative Infrastructure Solutions*, 9(3): 68. <https://doi.org/10.1007/s41062-024-01366-z>
- [12] Bureau of Indian Standards. (2013). IS 12269: Indian standard: Ordinary Portland cement, 53 grade—Specification (First revision). New Delhi, India: Bureau of Indian Standards.
- [13] Bureau of Indian Standards. (2016). IS 383-2016: Indian standard: Coarse and fine aggregate for concrete—Specification (Third revision). New Delhi, India: Bureau of Indian Standards.
- [14] Bureau of Indian Standards. (2003). IS 3812 (Part 2)-2003, Indian standard: Pulverized fuel ash—Specification: Part 2 for use as admixture in cement mortar and concrete (Second revision). New Delhi, India: Bureau of Indian Standards.

- [15] Bureau of Indian Standards. (2004). IS 9103: Indian standard: Concrete Admixtures-Specification (First revision). New Delhi, India: Bureau of Indian Standards.
- [16] ASTM International. (2022). Standard specification for slag cement for use in concrete and mortars (C0989/C0989M-18a). ASTM International. https://doi.org/10.1520/C0989_C0989M-18A
- [17] Bureau of Indian Standards. (2009). IS 10262-2009: Indian standard: Concrete mix proportioning—guidelines (First revision). New Delhi, India: Bureau of Indian Standards.
- [18] Bureau of Indian Standards. (2018). IS 1199-2018: Indian standard: Methods of sampling and analysis of concrete (Eleventh reprint November 1991). New Delhi, India: Bureau of Indian Standards.
- [19] Bureau of Indian Standards. (1959). IS 516-1959: Indian standard: Methods of tests for strength of concrete (Eighteenth reprint June 2006). New Delhi, India: Bureau of Indian Standards.
- [20] Sen, D., Alwashali, H., Islam, M.S., Seki, M., Maeda, M. (2023). Lateral strength evaluation of ferrocement strengthened masonry infilled RC frame based on experimentally observed failure mechanisms. In Structures. Elsevier, 58: 105428. <https://doi.org/10.1016/j.istruc.2023.105428>
- [21] Surendra, B.V., Ravindra, R. (2021). A study of affordable roofing system using ferrocement and bamboo cement panels. Journal of The Institution of Engineers (india): Series A, 102(3): 633-642. <https://doi.org/10.1007/S40030-021-00533-0>